PERGAMON

International Journal of Solids and Structures 38 (2001) 4293–4313

INTERNATIONAL JOURNAL OF SOLIDS and STRUCTURES

www.elsevier.com/locate/ijsolstr

High-resolution methods in vibratory analysis: application to ball bearing monitoring and production machine

J.P. Dron *, L. Rasolofondraibe, F. Bolaers, A. Pavan

Groupe de Mécanique Appliquée, Groupe de Recherche en Automatique et Mécanique Laboratoires d'Automatique et de Microélectronique, Université de Reims Champagne-Ardenne, IUT Leonard de Vinci, Rue des Crayéres, B.P. 1035, 51687 Reims Cedex 2, France

Received 10 October 1998; in revised form 15 June 2000

Abstract

This paper is concerned with the implementation of parametric spectrum analysis using a high-resolution technique for setting up a conditional maintenance program via vibration analysis on a forming press. To achieve this, the resolving power of signal-processing-based parametric techniques is illustrated using spectrum assessment computation. Processing of the experimental results enabled (i) various autoregressive (AR) spectrum analysis methods and especially Burg's algorithm to be tested and (ii) conventional spectrum analysis techniques such as the correlogram to be compared with parametric methods in terms of detection level as well as for mechanical component fault monitoring, especially ball bearing defects. Among various possible models, the AR model was retained along with Burg's algorithm and the Akaike information criterion. A detection and location methodology for faults likely to occur on rotating machinery was developed on the basis of the results that were obtained. The methodology, supplementing other analysis techniques, relies on the understanding of component spectrum behavior and various constraints, such as component access, spectral resolution of the industrial measuring device, and statistical properties of the power spectral density measurements of a random signal. The results show that parametric methods are particularly worthwhile in the early detection of component defects, especially when two characteristic frequencies are close to one another. However, the complexity of these techniques necessitates many precautions when they are implemented; consequently, they should not replace conventional methods, but supplement them.

Keywords: High-resolution methods; Vibration ball bearing; Correlogram; Forming press

1. Introduction

In order to be competitive, industry must, among other things, maintain manufacturing tools in perfect working order so as to reduce maintenance and repair delays as much as possible. To reach this goal, various maintenance policies may be considered, but the most rational is to implement a conditional maintenance policy. Such a policy is best based on analysis techniques and process monitoring and must be

* Corresponding author.
E-mail address: jp.don@univ-reims.fr (J.P. Dron).

0020-7683/01/$ - see front matter
PII: S0020-7683(00)00277-8

efficient and easy to implement. Among the different methods in use, machine vibration monitoring is presently the most widespread. This consists of monitoring, over time, the evolution of the vibratory signal of a mechanical system to assess the mechanisms of damage.

There exist several methods to characterize and monitor the condition of essential rotating machinery components. Among the kinds of vibration signal analyses and processing available, spectrum analysis has certainly been one of the most important and widespread in industry since Fast Fourier Transform (FFT) spectrum analyzers made their appearance. However, the resulting spectrum is too rich in sinusoidal components blurred with parasitic noises, which often makes it difficult to exploit the information contained in the obtained spectra. Moreover, most industrial measuring devices have limited signal acquisition capabilities (predefined frequency range, limited sample number, etc.). Thus, it becomes difficult to distinguish characteristic frequencies that are close together. Therefore, more efficient analysis techniques, which can distinguish very closely spaced sinusoidal signals independent of the resolving power of the measuring device, are required.

In this paper, an experimental procedure concerned with fault monitoring, characterized by a spectrum containing quasi-identical components giving very close characteristic frequencies, is provided. This procedure is based on the use of an autoregressive (AR) spectrum analysis along with Burg's algorithm and the Akaike information criterion (AIC). Various constraints, such as fluctuations in vibration level, sensor position, and measuring parameters, such as frequency range and sample number, were taken into account to select suitable measurement and analysis technique(s).

An industrial implementation of damage monitoring of sensitive components of a forming press, which relies on a judicious choice of vibration monitoring conditions and on the use of the "high-resolution" analysis technique to supplement conventional analyses, is presented. Conventional analyses in the time domain include RMS value and kurtosis and in the frequency domain, envelope and spectrum analyses.

2. Implemented signal analysis methods

Research has been undertaken to highlight and monitor damage to mechanical components of rotating machinery. When a complex or well-guarded machine, such as a forming press, is to be monitored, it is often difficult to position the sensor near every component of interest. Therefore, several components are often monitored from the same sensor position. The resulting acquired signal contains and displays the vibration signature of all components sensed simultaneously. The use of more effective techniques is required to enable more efficient machine fault diagnosis (Baillie and Mathiew, 1996).

2.1. Conventional techniques

Together with the traditional AR parametric spectrum analysis method, a conventional spectrum assessment technique was implemented. It was then possible to compare these techniques and to highlight the contribution of the former during the early stage of fault detection and monitoring. The conventional method is based on the use of a Fourier transform of the vibration auto-correlation function in association with a Hanning weighting window (correlogram) and is defined in the following equation:

$$S_x(f) = r(0) + 2\sum_{p=1}^{N-1} r(p)\cos(2\pi pf), \tag{1}$$

where $r(p)$ denotes the assessment of autocorrelation coefficients.

2.2. The autoregressive spectrum analysis method

Parametric spectrum analysis methods were defined and developed in the frequency domain to obtain power spectral density resolution beyond that possible using conventional methods based on the Fourier transform (Kay and Marple, 1981). These methods, known as high-resolution techniques, have numerous applications and have been applied recently to the vibration analysis of rotating machinery (Mechefske and Mathiew, 1992).

Parametric spectrum analysis methods rely on time modeling the signal. The modeling is based on the assumption that the observed signal is generated by the action of a linear filter on white noise. The spectrum analysis problem then reduces to the identification of the filter model, for which the number of parameters is obtained by minimizing the error between the measured signal and the output of the model according to an optimality criterion (Akaike, 1974). The power spectral density is then computed from the recorded model.

The class of parametric methods that provides the model of a random process with an autoregressive moving average (ARMA), an AR, or a moving average (MA) type model is among the most conventional and above all the most widely used in vibration analysis (Kay and Marple, 1981). The major problems encountered when implementing parametric spectrum analysis methods are a result of the choice of (i) the model for representing the vibration signal, (ii) the computing algorithm for the model parameters, and/or (iii) the model order selection criterion, i.e., the number of its parameters since it is a polynomial model.

Among signal representation models, the AR model was chosen here since it is the best compromise between temporal representation and speed, efficiency and simplicity of algorithms for computing the model parameters. The AR model is currently being used for the detection of the most common mechanical defects via parametric spectrum analysis. Besides highlighting characteristic frequencies associated with rotating machinery, AR modeling allows the detection of the presence of local non-stationarities in the vibration signal as a result of linear prediction errors (Baillie and Mathiew, 1996). These non-stationarities indicate component defects in many cases, such as those found in a geared system (Drouiche and Sidahmed, 1991).

The AR model is provided with the following recurring equation:

$$e(n) = y(n) + \sum_{i=1}^{p} a_i y(n-i), \tag{2}$$

where $e(n)$ represents the linear or residual prediction error, a_i represents the model parameters, $y(n)$ represents the sensor output value.

The a_i parameter value is obtained via the solution of a linear equation system, the so-called Yule–Walker equations, which depict the relationship between model parameters and signal correlation coefficients (or correlation matrix/array). Yule–Walker equations can be obtained either with the maximal entropy condition or via a linear prediction method. Burg's algorithm enables model parameters to be assessed directly from the observed data without requiring the intermediate step of correlation matrix assessment. Burg's algorithm is based on the arithmetic mean of direct and regressive prediction error powers. The direct prediction error is defined by

$$e_m^f(n) = x(n) + \sum_{i=1}^{m} a_{m,i} x(n-i). \tag{3}$$

The regressive prediction error is provided by

$$e_m^b(n) = x(n-m) + \sum_{i=1}^{m} a_{m,i} x(n+i-m). \tag{4}$$

By introducing Levinson's recurring principle in the definition, error recurring relations are obtained:

$$e_m^f(n) = e_{m-1}^f(n) + K_m e_{m-1}^b(n-1), \tag{5}$$

$$e_m^b(n) = e_{m-1}^b(n-1) + K_m e_{m-1}^f(n). \tag{6}$$

Burg's criterion is the arithmetic mean of direct and regressive prediction error powers:

$$C_m = \frac{1}{2(N-p+1)}\left[\sum_{n=m}^{N}\left(\left|e_m^f(n)\right|^2 + \left|e_m^b(n)\right|^2\right)\right]. \tag{7}$$

By introducing Levinson's recurring principle in the definition, the following error recurring relations are obtained: Burg's criterion is the arithmetic mean of the direct and regressive prediction error powers.

By replacing and with relations (5) and (6), e_m becomes a single K_m parameter function, for at the mth order prediction, errors at $m-1$ are known. Resetting the C_m derivation with respect to K_m provides the C_m assessment.

$$K_m = -\frac{2\sum_{n=m}^{N} e_{m-1}^f(n) e_{m-1}^b(n-1)}{\sum_{n=m}^{N}\left(\left|e_{m-1}^f(n)\right|^2 + \left|e_{m-1}^b(n-1)\right|^2\right)}. \tag{8}$$

Therefore, the algorithm is as shown in Scheme 1.

Here, N is the number of samples, m, the recursive iteration number, and T_e, the sampling time.

Other techniques, such as Capon's technique or the least recurring square method to mention some of the more conventional ones, were implemented on other rotating machinery. Thus, the understanding of parameters and model order enables the computation of power spectrum density through the following relation:

$$P(f) = \frac{1}{|A(f)|^2} = \frac{\sigma_e^2}{\left|1 + \sum_{i=1}^{p} a_i \mathrm{e}^{-2j\pi f T_e}\right|^2}, \tag{15}$$

where a_i denotes the AR filter coefficients, σ_e, the white noise variance, p, the AR model order, and T_e, the sampling time.

Contrary to results obtained using conventional techniques, the power spectral density recorded using AR methods did not permit a good assessment of the spectrum amplitude. However, the advantage of the AR method lies in its ability to detect defects early as well as its ability to resolve two closely spaced frequencies; hence, its importance in conditional maintenance.

It must be borne in mind that the accuracy obtained when recording an AR spectrum essentially depends on the number of AR model parameters used (called the model order of the filter). If the selected order is too low, then the spectrum is smoothed and some information is lost; consequently, the method is no longer one of high resolution. On the other hand, if the model order is too high, spectrum lines with no physical meaning appear (Robert and Mailhes, 1994). This may be misleading and cause a diagnosis error.

Two order selection criteria were retained: the final predictor error (FPE) (16), the AIC (18) and the minimum description length (MDL) (19). These criteria, based on prediction error power, were developed by Akaike (1974). The prediction error power monotonically decreases with filter order whereas assessed variance increases with order. Prediction error-based criteria tend towards a compromise between error power and variance.

The FPE criterion is

$$\mathrm{FPE}(p) = V_p \frac{N+p+1}{N-p-1}, \tag{16}$$

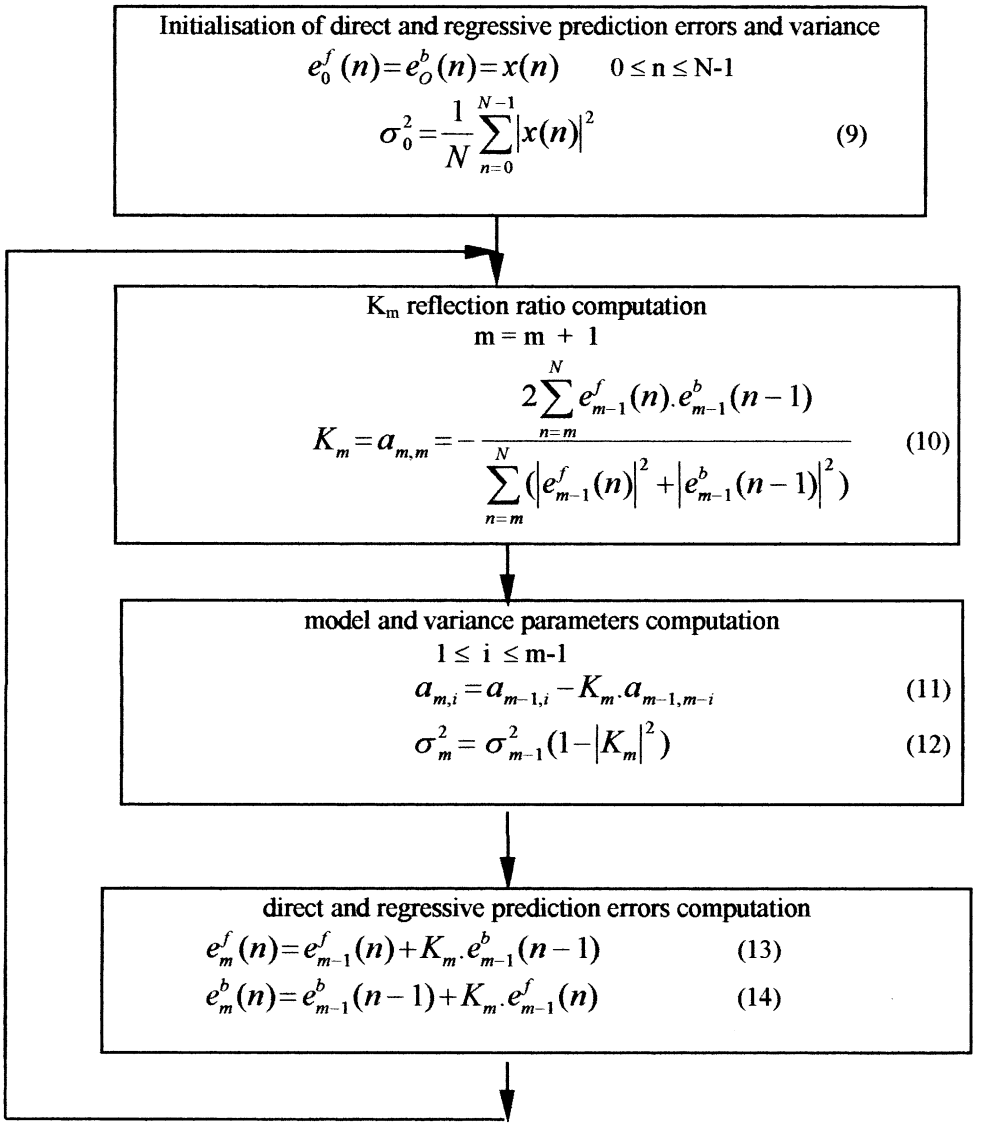

Scheme 1.

where

$$V_p=\frac{\sigma_p^2}{r_{xx}(0)}=\prod_{i=1}^{p}\left(1-|K_i|^2\right), \tag{17}$$

where V_p denotes variance of the standardized prediction error, and N, the number of samples (time data).

The AIC is

$$\mathrm{AIC}(p)=N\ln(V_p)+2p. \tag{18}$$

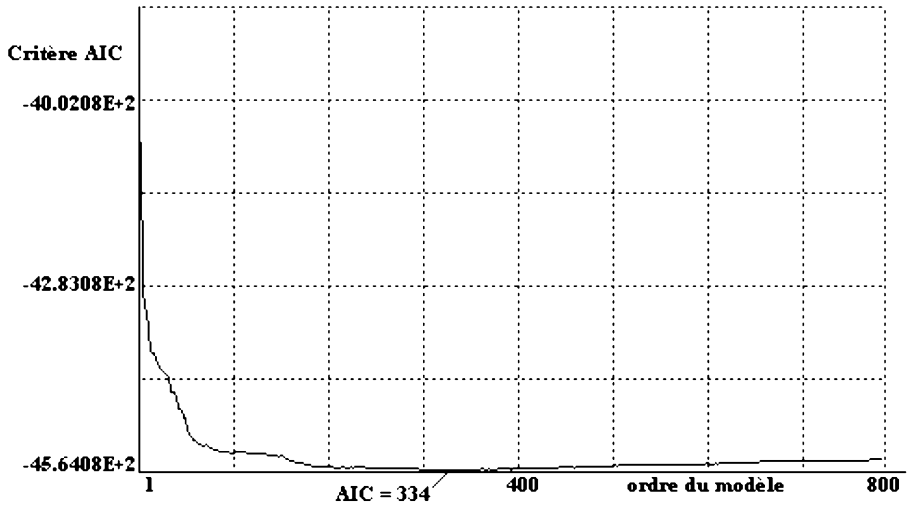

Fig. 1. Determination of the model order using the AIC criterion (number of samples: 2048 and frequency range: 100 Hz).

The MDL criterion (proposed by Rissanen) is

$$\mathrm{MDL}(p) = N \ln(V_p) + p \ln(N). \tag{19}$$

The first term of the AIC criterion is proportional to the maximum likelihood of model-assessed parameters and the second term is a bias correction. The FPE criterion is viewed as the sum of the unpredictable part of the variance of the observation process and a quantity representing the assessment inaccuracy of the AR parameters. Research has recently been undertaken on the study and comparison of various AR model order selection criteria (Dickie and Nandak, 1994). The AIC criterion was retained for the experimental work reported here for it enabled a reasonably accurate assessment of the required number of AR model parameters whereas the FPE criterion overestimated the model order.

The optimum model order will minimize these criteria. Fig. 1 illustrates the determination of the model order using the AIC for a number of samples and a specified frequency range. This criterion was obtained using a vibration signal from a forming press.

3. Experimental validation of autoregressive spectrum analysis methods on a bench test

3.1. Bench test and instrumentation specifications

The monitoring of ball bearing damage was achieved through regular monitoring of 13 ball bearings mounted on a single shaft between the chuck and the tailstock of a horizontal lathe (Fig. 2). The outer rings of the bearings were blocked rotationally via a simple assembly (a clamping screw). Furthermore, a small round sticker was stuck on each outer ring perpendicular to the shaft axis so as to facilitate the measurements.

For the arrangement described, a single sensor enabled serial monitoring according to a radial direction of the bearing damage. In addition to the accelerometer, the measurement chain incorporated an industrial FFT analyzer with limited characteristics (displayed frequency range, maximum number of samples limited to 4096) linked to a microcomputer via an IEEE 448 interface that enabled the analyzer to be controlled

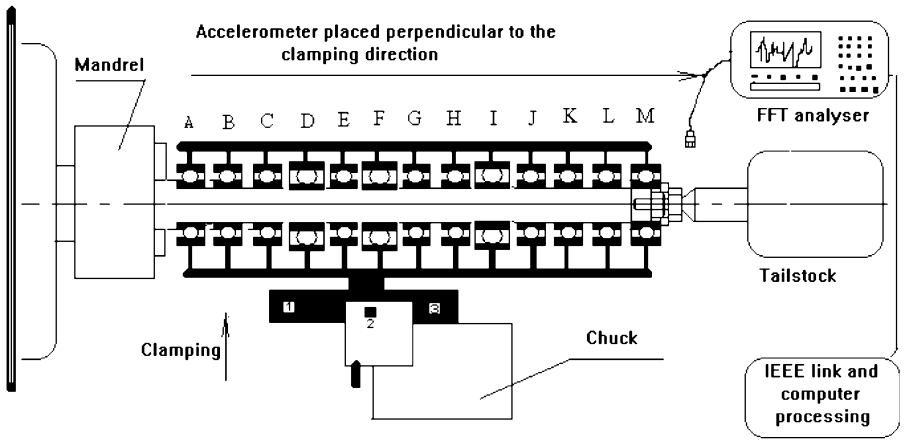

Fig. 2. Measuring bench and monitoring device. The 10 6002 SNR bearings are labeled A, B, C, D, E, F, G, H, I, J, K, L, M, and the three 6202EE bearings D, F, I.

from the computer. The analyzer was only used for the acquisition of the signal in the time domain, while the other processing was carried out using a microcomputer and the custom-built item of software.

Three other sensor positions were chosen (Fig. 2: positions 1–3) to study the propagation of the vibrations emitted by mechanical components on the one hand, and on the other hand, to record the various characteristic frequencies representing bearing faults using a single sensor. This enabled the determination of suitable detecting methods as a function of sensor position.

3.2. The different types of faults occurring in a ball bearing

Two types of defects are likely to occur in a ball bearing:

1. Defects evenly distributed on the active parts of the bearing, essentially due to bearing manufacture (geometrical defects of elements, defect of contact surfaces): These defects can only be detected via temporal methods. Such methods use statistical or energy parameters e.g. kurtosis, RMS value, defect factor, or other methods in the time domain (Pachaud and Fray, 1997).
2. Defects located on elements being part of bearings, such as flaking, indentation, jamming: These are characterized by repetitive shocks that occur whenever a rolling element encounters the defect. Each located defect is identified by a recurring frequency that depends on the geometrical characteristics of the bearing and its rotational frequency.

If a defect is localized on the outer ring race, a recurring frequency shock appears at each ball pass (20) as follows:

$$f_e = \frac{n}{2}\frac{N}{60}\left(1 - \frac{d}{D}\cos\theta\right). \tag{20}$$

Similarly, a defect located on the inner ring is characterized by a particular vibration frequency:

$$f_i = \frac{n}{2}\frac{N}{60}\left(1 + \frac{d}{D}\cos\theta\right). \tag{21}$$

If a defect is located on a rolling element, its characteristic vibration frequency will be

Table 1
Characteristic fault frequencies of ball bearing 6002 and 6202

Bearing specifications	6002 bearing	6202 bearing
Average diameter (mm)	23.5	25
Ball number	9	8
Ball diameter (mm)	4.7	6
Contact angle (°)	0	0
Inner ring speed (rpm)	945	945
Outer ring speed (rpm)	0	0
Defect localized on the outer ring (Hz)	56.7	47.8
Defect localized on the inner ring (Hz)	85.05	78.12
Defect localized on a rolling element (Hz)	75.6	61.84

$$f_b = \frac{D}{d}\frac{N}{60}\left(1 - \left(\frac{d}{D}\cos\theta\right)^2\right), \tag{22}$$

where n, N, d, D, q, respectively, denote ball number, shaft rotational speed (rpm), ball diameter, average diameter, and contact angle, respectively.

Frequency domain techniques are the most efficient for fault monitoring since they allow both the detection of defects and the monitoring of their propagation (Table 1).

3.3. Experimental results

In this section, identified defects on bearing moving parts (flaking, strain, indentation) are given particular attention. Clamping the bearing, which was achieved via a screw/bolt on the outer ring, allows a specified load to be applied in a given direction. The generated stress, in turn, causes surface fatigue failure at two given points on the ring. This causes the appearance of an indentation, the evolution of which explains the higher vibration level at a characteristic outer-ring-linked-defect frequency (Fig. 3).

3.3.1. Experimental results analysis on the 6002 bearing

The experimental work consisted of monitoring the evolution of the spectrum for each bearing over a period of time, and in particular, the amplitude of the frequencies that characterize the localized defects. This evolution is characterized by (i) an increase in the overall vibration level, (ii) the appearance of

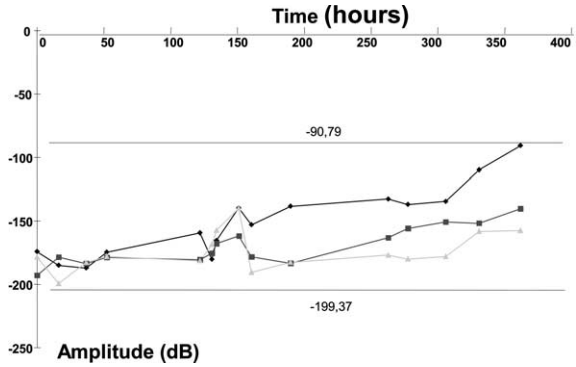

Fig. 3. Evolution of the frequency amplitude spectrum for bearing A defects.

harmonics that characterize different fault frequencies, and (iii) the appearance of other phenomena, such as modulation. Fig. 3 displays the evolution of the spectral curves, assessed by AR parametric spectrum analysis, showing the frequencies that are characteristic of a bearing defect.

Initially, both (conventional and parametric) analysis methods give a fault-free spectral signature for each bearing. Despite the similarity of the spectra obtained using the two methods, the overall amplitude differs between spectra as both techniques do not possess the same statistical characteristics. Moreover, for a judiciously selected model (depending on the order selection criterion and the sample number), the AR spectrum reveals all the periodic phenomena contained in the vibratory signal. Thus, only the axle rotational speed (fr = 15–75 Hz) and all of its harmonics ranging from 0 to 100 Hz can appear in each bearing spectrum. The other peaks correspond to the lathe dynamic response peaks.

After 200 operating hours, each spectral curve regularly increases in amplitude, particularly for the 6002 bearing outer ring defect. The parametric spectrum reveals the characteristic groove of a fault localized on the outer ring (Fig. 4). As a result, the first signs of damage to the outer ring can be assumed to exist. However, even though the peak seems very high at this frequency, nothing can be concluded about the fault seriousness. The corresponding amplitude varies only a little compared to the previous values, as the evolution of the spectral curve shows. As far as monitoring is concerned, it is the rate of increase in amplitude of a spectral peak that provides information on the health condition of a component, not the single value at a specific time.

On the one hand, the conventional spectrum (correlogram) of the A bearing does not display the signs of a defect after 200 operating hours (Fig. 5). This is not a spectrum resolution problem since the selected measuring parameters were computed so as to enable the localization of characteristic bearing fault lines.

The conventional spectrum does not highlight the overall variations of the low amplitude characteristic lines. The amplitude of the third harmonic is much higher than the amplitudes of characteristic close frequencies.

The p order of the AR model steadily increased as time passed. This can be explained by the fact that the number of characteristic spectrum lines increases as the bearing deteriorates. In fact, the number of model parameters is strongly linked to the number of periodic signals contained in the vibration signal. The model is determined for a given operating condition at a given time. When the bearing deteriorates, the previous model cannot be adapted to the new condition. Thus, it is redefined anew.

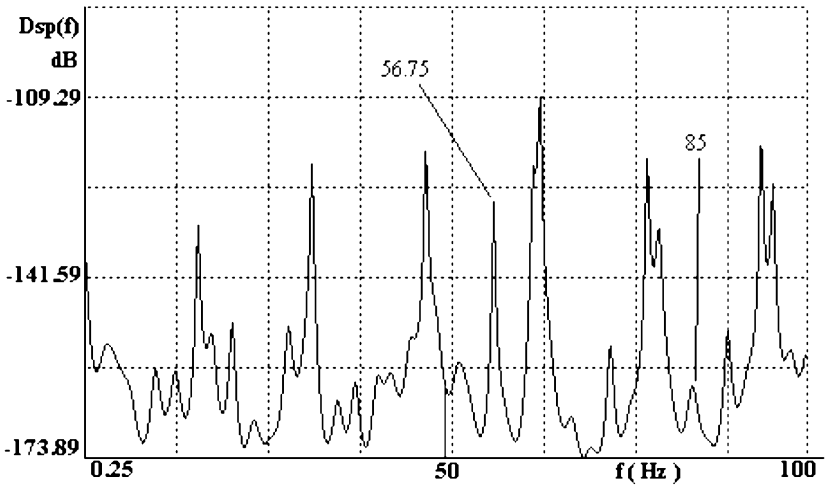

Fig. 4. Spectrum for bearing A after 200 operating hours [1 1 0], showing the appearance of a defect located on the outer ring (56.75 Hz).

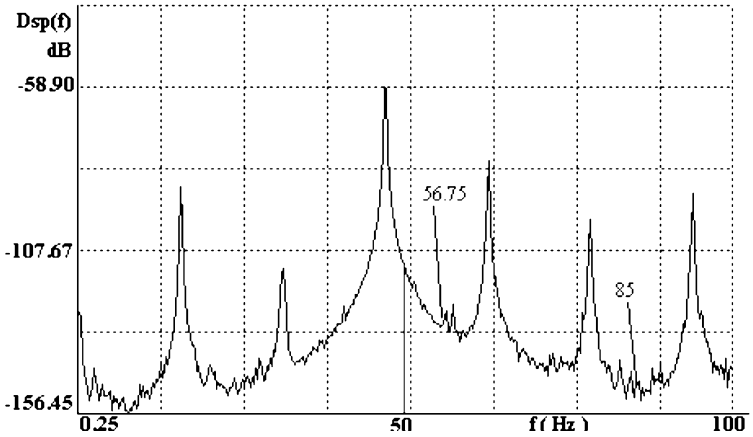

Fig. 5. Conventional bearing A (correlogram) after 200 operating hours.

Among the three selection criteria of the selected order, the AIC seems to be the best to assess the number of parameters for the AR model. The MDL criterion often underestimates the model order, whereas the FPE overestimates it. These order selection criteria do not possess the same statistical properties, and most of the time, the important decrease of the signal to noise ratio may result in an overestimation of the AR model order, whatever criterion is used. That the retained model order does not correspond to the exact model order but is close, does not mean a strong variation in the level of the overall amplitude of the computed spectrum. A close to minimum p value can then be retained via the order selection criterion.

3.3.2. 6202EE bearings (D, F, I) experimental analysis

The time history curves of the SNR bearings with the 6202EE reference number have features that are analogous to the 6002 bearings as shown in Fig. 6.

As in the previous case, at the beginning (for conventional or parametric analyses), bearing F spectra only display the output shaft rotational speed (fr) and its harmonics as well as the lathe dynamic response frequencies. All of the phenomena previously described for the 6202EE bearings are encountered again.

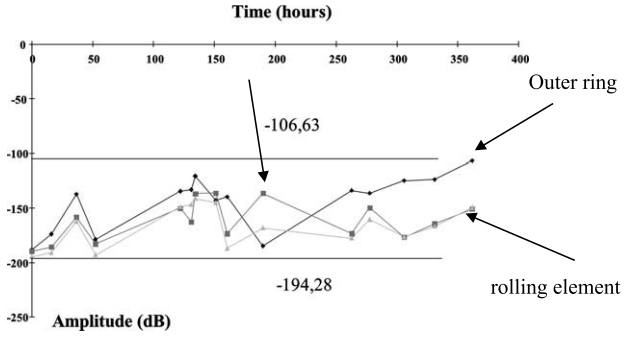

Fig. 6. Variation with time of the characteristic frequency amplitudes for the bearing F defects.

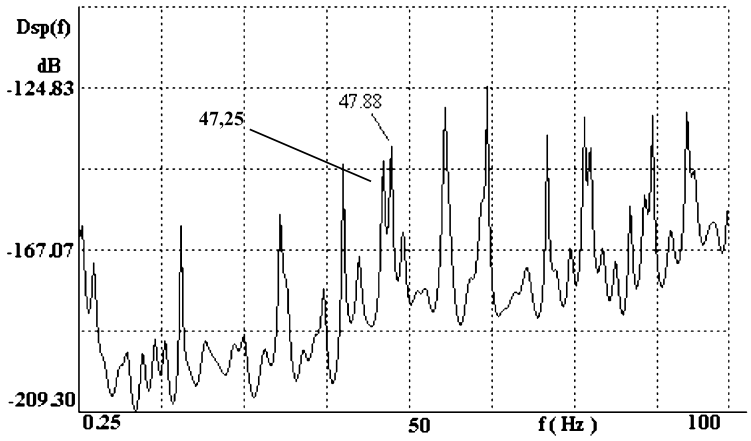

Fig. 7. Bearing F parametric spectrum after 350 operating hours. Note the appearance of the peak at 47.88 Hz due to the outer ring defect.

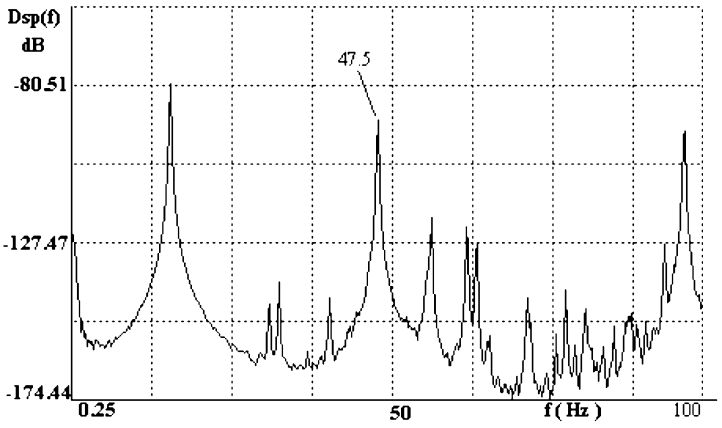

Fig. 8. Conventional bearing F spectrum after experimental testing.

The amplitude of each characteristic fault frequency of the 6202EE bearing varies about an average value (about 160 dB, Fig. 6) for the 0–200 operating hour period. The amplitude begins to increase after 200 h and it is more noticeable for the frequency corresponding to a defect localized on the outer ring (47.88 Hz). The parametric spectrum (Fig. 7) reveals the first signs of this defect. On the other hand, the conventional correlogram-type spectrum (Fig. 8) displays a dynamic problem linked to the spectrum line width. This problem is even greater for 6202EE bearings since the third harmonic of the output shaft rotational speed (47.25 Hz) is very close the localized defect characteristic frequency on the outer ring (47.88 Hz). The same problem applies to the fault located on the inner ring, characterized by a frequency of 78.12 Hz, while the fifth harmonic of the shaft rotational speed (15.75 Hz) is at 78.75 Hz.

In summary, parametric spectral assessment techniques are high-resolution methods and thus enable the detection of the first signs of a fault in a mechanical component. Such techniques may complement conventional methods based on the Fourier transform that still remain the easiest to implement when the

component vibratory signature is not characterized by defect frequencies that are so close together that they cannot be distinguished separately.

3.3.3. Experimental results from the three sensor positions (1–3)

The sensor was placed in three different positions (Fig. 2, positions 1–3) to study the propagation of vibrations emitted by various mechanical components and to recover the entire set of characteristic fault frequencies for different bearings types. This study is essential in so far as (i) each sensitive rotating machinery component is not accessible via a sensor, and (ii) it is necessary to reduce the monitoring chain installation cost by reducing the amount of sensors. It is important to point out that time domain analysis techniques are no longer suitable for bearing damage monitoring since the vibratory signal obtained represents the vibratory signature of the whole component set. Hence, only frequency analysis enables the detection and the monitoring of the (6002 and 6202EE) bearing damage progression. Whatever the spectrum assessment in use, the 10 6002 and the three 6202EE bearings display the same frequencies that are characteristic of localized faults; thus, it is extremely difficult to identify the bearing(s) on which a defect appears. Bearing vibratory signatures have different wavelengths, but in terms of frequency localization, faults are blurred for each of the types.

The amplitude corresponding to each localized defect characteristic frequency is the output of the superposition of the vibratory signatures of the 13 bearings when these faults are present. The time history spectral curves for both types of bearing with the sensor placed in position 1 or 3 evolve in the same way as those obtained when the sensor is placed on each bearing (Fig. 9).

The most prominent defects on the outer ring, located at 56.75 Hz for the 6002 bearing and at 48 Hz for the 6202EE, are present with equivalent respective amplitudes on positions 1 and 3, positions that are symmetrical on the chuck (Figs. 10 and 12). The corresponding amplitudes representing the defects are significantly reduced in the recording for position 2 (Fig. 11) where the sensor is placed on the chuck that to some extent isolates the vibrations.

The study of the vibration propagation phenomenon in a machine frame is thus important. The understanding of these phenomena allows the determination of ideal sensor positions likely to record a maximum of information. It is actually useless to develop high-resolution spectrum analysis methods if the information is recorded in a position where it is masked, as shown in the results for position 2 for instance.

To conclude, good sensor positioning is essential; however, the problem of detection of faults localized on two identical bearings cannot be solved with these methods.

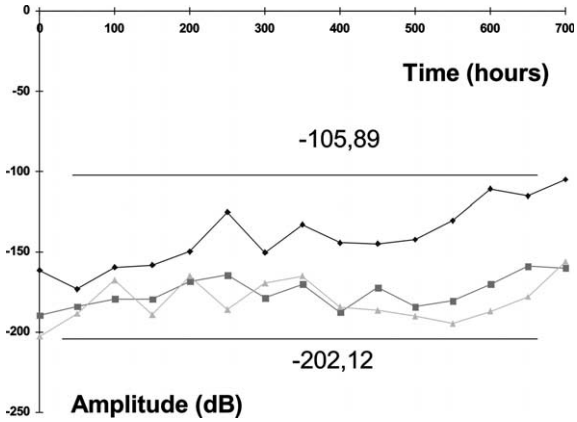

Fig. 9. Frequency spectrum evolution at position 1 for a bearing with a fault.

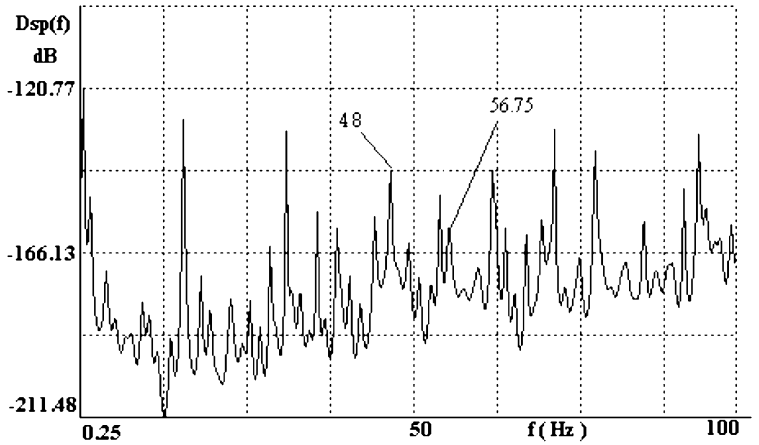

Fig. 10. AR spectrum after 150 operating hours recorded by the sensor in position 1. The appearance of the defect is localized on the outer ring.

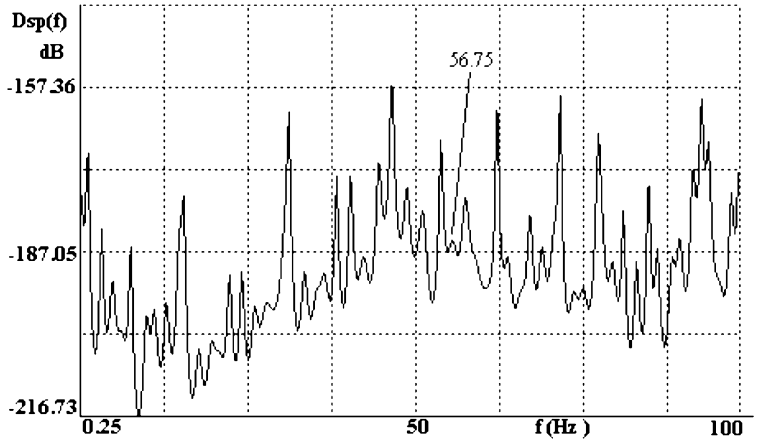

Fig. 11. AR spectrum after 150 operating hours recorded by the sensor in position 2. The amplitude of the defect localized on the outer ring is low.

3.4. Discussion

The frequency analysis described previously has demonstrated the benefits of the AR spectrum (Figs. 10–12) techniques over conventional ones (correlogram). Burg's algorithm-based parametric spectrum assessment allows early damage detection and fault evolution monitoring of bearings. This is because this technique detects all of the recurring phenomena contained in a vibratory signal. It is a high-resolution method that also reduces background noise in the spectrum, thus allowing bearing faults to be detected more quickly.

The amplitude differences between the correlogram and the parametric spectrum are linked to the algorithms used for spectral computations. Indeed, spectrum assessment based on the AR pattern reduces background noise so as to highlight the signal's recurring phenomena. This implies amplitude averaging at all frequencies of the parametric spectrum. Such averaging accounts for the amplitude differences between

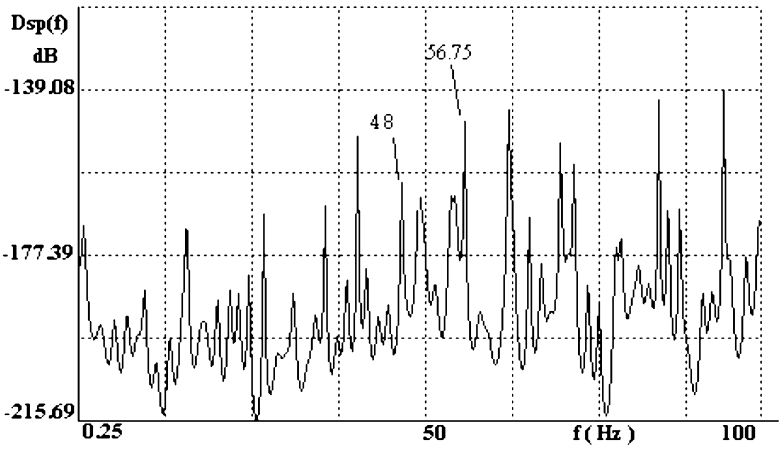

Fig. 12. AR spectrum after 150 operating hours recorded by the sensor in position 3.

the correlogram and the parametric spectrum. Hence, the spectrum amplitudes stemming from both methods have not been compared as the aim was to highlight the presence of defect frequencies in noisy spectra. The resolution power of the parametric spectrum, which made it possible to distinguish two close frequencies, has been established (compare Figs. 7 and 8). Model order selection has also been shown to be important. The model order cannot be over or underestimated since this might result in significant errors in the spectral computations and a completely incorrect interpretation of the results.

Finally, emphasis has been placed on the possible ability of these high-resolution methods to recover the vibratory signature of a large set of monitored components with a small number of judiciously placed sensors. These complex techniques are not intended to replace conventional methods, but rather to complement them. In particular, for the case of components characterized by identical defect frequencies, the identification of the defective component cannot be achieved without using complementary analysis techniques.

Here, AR spectrum analysis has been implemented on a forming press, the unexpected failure of which would result in a substantial financial loss. Results of this work are discussed in Section 4.

After dismantling the various elements, we found faults neither on the inner ring nor on the rolling parts. However there were faults on the outer ring. This can be accounted for by the fact that the ring is fixed and two of its points undergo heavier strain than the other ones. They are the points where the screws make contact with the outer ring. The strain entails wear which then leads to faults in the ring.

4. Implementation of parametric techniques on a forming press

4.1. Forming press kinematics study

The study focuses on a swan-neck forming press with a 125 ton capacity (Fig. 13). The press consists of a frame that drives the shaft through two plain bearings (bronze rings). This shaft acts as a cam in order to convert a rod/strut continuous rotational motion into an alternative rectilinear motion. The shaft also drives the flywheel through a belt-based system. The shaft's rotational motion is transmitted via a temporary coupling of the friction gear type. It is slowed down and halted using a friction brake. The press has

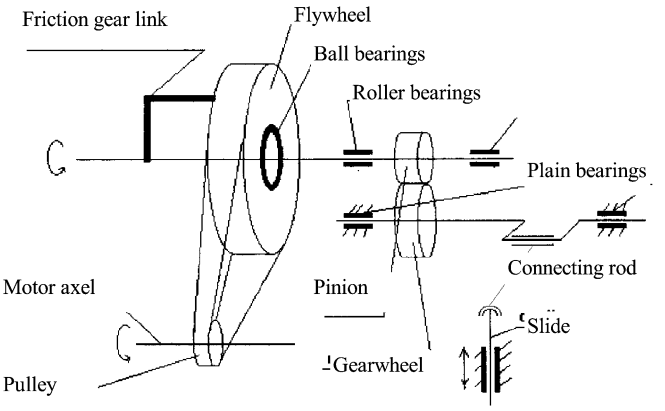

Fig. 13. Two axle press.

two periodic operating modes and an ad hoc operating mode. For this study, research was limited to the two periodic modes in which the press behaves like a rotating machine.

4.1.1. Waiting mode

In this mode, one gear is not excited; only the flywheel, the driving belt and the motor are operating. The flywheel is free to rotate on the primary shaft and the brace slide set is inserted. In these conditions, only the motor (6), the driving belt (3), the flywheel (8), and the flywheel/primary shaft link ball bearing (9) can be monitored (Fig. 14).

4.1.2. Continuous mode

Here, the gear is excited, and all parts are moving. The press behaves similar to a rotating machine and the dynamic stress is periodic. The flywheel drives the brace rotationally through the pinions (1) and (10). The brace imposes an up-and-down movement to the slide that contains the forming tool. For this operating mode, motion transmission devices (belt, pinion) as well as bearings (fluid bearing (5), roller bearings (2) and (4)) can be monitored (Fig. 14).

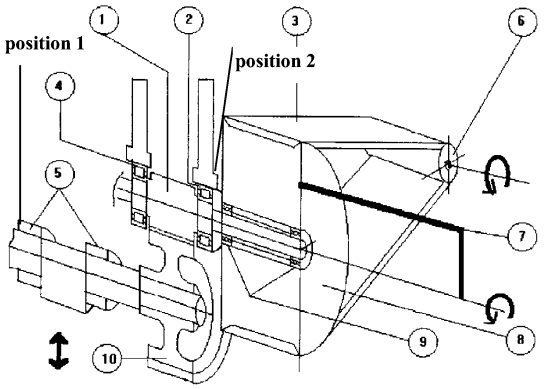

Fig. 14. Press driving line.

4.2. Problem formulation

The experimental problems encountered were (i) the selection of accelerometer mounting positions for an accelerometer in order to recover as much information as possible, (ii) the optimal motor rotational speed to enable the best localization of typical mechanical parts faults, and (iii) the characteristic device frequencies that can be monitored.

The choice of the accelerometer locations is guided by the accessibility of machine components to be monitored as well as the propagation of frame vibrations. The restriction linked to component accessibility has led to the consideration of two positions: close to the flywheel (position 1), which enables the monitoring of components linked to the primary shaft and the flywheel; and close to the slide (position 2), so as to monitor particularly the components linked to the brace (pinion, fluid bearings).

Forming presses are machines with low shaft rotation speeds. The press that was the object of this study had two conical roller bearings with almost identical technical features, resulting in very close characteristic frequencies. As they were located very close to each other, the monitoring of the two bearings could only be achieved using the same spectrum. The characteristic frequencies were dependent on the bearing size and shaft rotational speeds; the most suitable speed for defect identification was also the highest. When the motor rotational speed increased, the interval between two characteristic component defect frequencies increased, thus allowing each characteristic frequency in the spectrum to be displayed more clearly and allowing all the characteristic frequencies to be revealed in the spectrum. However, by increasing motor rotational speed, it is necessary to increase the useful frequency range of the measuring apparatus when acquiring the vibratory signal, which tends to reduce spectrum resolution. Therefore, a good compromise between rotational speed and spectrum resolution needs to be determined so as to optimize the measurements. This involves determining ideal press rotational speeds together with the most appropriate spectrum analyzer settings for signal acquisition.

Characteristic fault frequencies and excitation source analysis according to motor rotational speed enables the following to be specified: (i) the number of samples to take, (ii) the frequency range of the analysis, and (iii) the motor rotational speed in order to obtain optimal spectral resolution.

When the press is in standby mode the characteristic frequencies that can be monitored correspond either to motor shaft and flywheel unbalances, to belt motion, or to flywheel/primary shaft link rolling bearings. For an 80-rpm motor shaft rotational speed, characteristic fault frequencies are listed in Table 2.

Table 2
Characteristic fault frequencies of the component forming press

Component	Typical frequencies defect	Output shaft speed (Hz)	rpm	Numbering samples	Frequency range	Sensor position
Motor shaft	Unbalance	45.07	80	1024	50	1ne80
Flywheel	Unbalance	7.12	80	1024	50	1ne80
Belt	Driving	5.20	80	1024	50	1ne80
Bearing 6220	Inner ring defect	42.04	80	1024	50	1ne80
Bearing 6220	Outer ring defect	29.13	80	1024	50	1ne80
Bearing 6220	Roller element defect	37.93	80	1024	50	1ne80
Bearing 22 222	Inner ring defect	50.71	70	4096	100	1em70
Bearing 22 222	Outer ring defect	67.09	70	4096	100	1em70
Bearing 22 222	Roller element defect	49.54	80	4096	50	1em50
Bearing 23 222	Inner ring defect	50.80	70	4096	100	1em70
Bearing 23 222	Outer ring defect	67.00	70	4096	100	1em70
Bearing 23 222	Roller element defect	49.57	80	4096	50	1em50

The main advantage of using parametric methods is that it enables two characteristic frequencies, which cannot be detected by conventional methods, to be distinguished. The machine studied here did not enable the establishment of this property as neither bearing (22 222 and 23 222) was damaged (frequencies 49.54 and 49.57 Hz).

4.3. Results

Given the number of mechanical components to be monitored on the press, the recorded vibration signal spectrum is very rich. Moreover, each characteristic fault frequency generates harmonics, the number of which depends essentially on the nature and seriousness of the localized defect. However, these harmonics cannot be interpreted to characterize a component defect since the appearance and disappearance of some harmonics occurs randomly and depends on several factors (rotational speed variation, external parasitic effects, etc.). Only spectral amplitude evolution monitoring at the characteristic fault frequencies remains efficient when characterizing component faults. To stress the contribution of AR parametric methods to fault detection, three recordings are presented that display the evolution of various faults localized on press components. These three recordings correspond to the waiting mode, where the sensor is placed in position 1. Theoretically, in these conditions, six characteristic fault frequencies should be detected were the components to be monitored damaged or on the verge of sustaining damage (Table 2).

4.3.1. Recording 1

From the first recording, the major differences between the two (conventional and parametric) techniques have been highlighted in terms of the localization of characteristic component defects. Flywheel unbalance (7.12 Hz) is detected in the conventional spectrum (Fig. 15) with an amplitude of 158.54 dB. This defect generated three frequencies in the spectrum.

Theoretically, the characteristic frequency of the 6202EE ball bearing defects is around 37.93 Hz. The 37.25 Hz peak in the spectrum could then be considered as a bearing ball defect but the next measure would need be awaited to identify the exact position of the rolling element fault frequency. Note that the 100 Hz range has been preferred to the 50 Hz range. To offset this difference, 2048 samples were taken instead of 1024. The presence of other peaks, which are not harmonics or modulations, has been ignored.

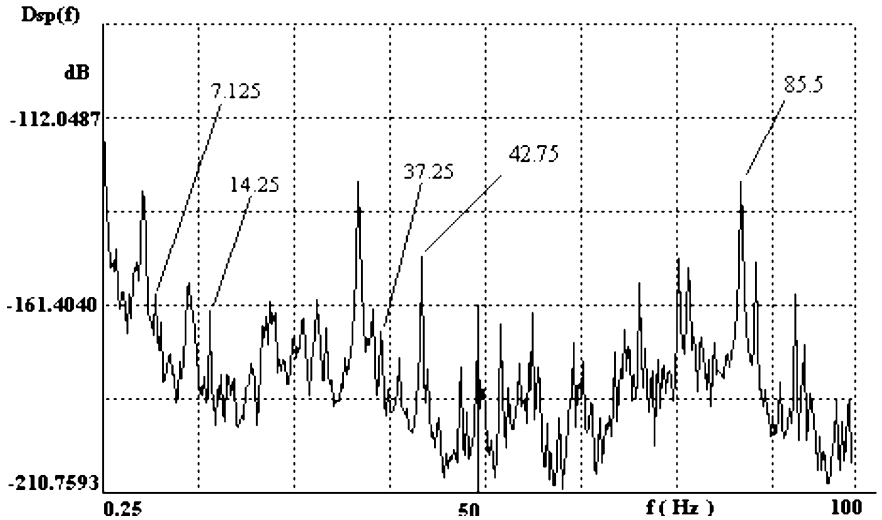

Fig. 15. Conventional spectrum (correlogram).

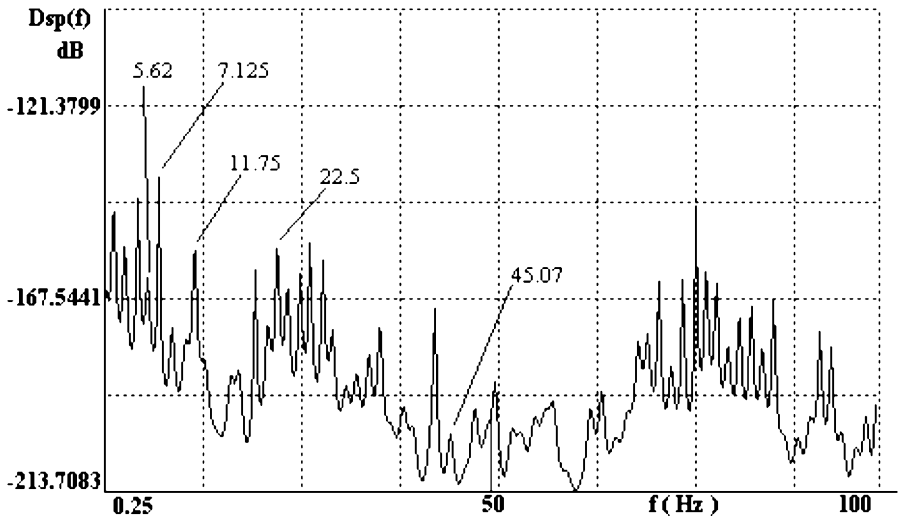

Fig. 16. AR spectrum (p order = 170 via the AIC).

In the AR spectrum (Fig. 16), on the other hand, the presence of flywheel unbalance at 7.12 Hz and the motor shaft rotational speed at 45.07 Hz, which cannot be detected on the conventional spectrum, can be seen. The presence of two harmonics (harmonic 1: 11.75 Hz (−126.2 dB) and harmonic 2: 22.5 Hz (−122.43 dB)) indicates the presence of a belt-driving fault. No peak corresponding to the characteristic fault frequencies of the 6202EE bearings is detected, which indicates that there is no damage. However, it is worth noting that Burg's algorithm is sensitive to spectral noise effects and that model order selection plays an important part in revealing all of the recurring phenomena. This is one of the major problems related to signal parametric modeling.

4.3.2. Recording 2

The results obtained do confirm those previously recorded. As for recording 1, flywheel unbalance amplitude increases and a belt-driving fault appears at 5.62 Hz (Fig. 17). Motor shaft unbalance does not appear on the conventional spectrum. There is no significant peak of the 6202EE bearing condition. All this indicates that it is still in perfect working order.

However, in the parametric spectrum (Fig. 18), a 6220 roller bearing element fault begins to appear and is characterized by a 38 Hz peak. This confirms the usefulness of parametric techniques in early fault detection, but the same previous phenomena are still encountered.

4.3.3. Recording 3

On the basis of the previous recordings in the same mode, Fig. 19 shows that the 6220 bearing outer ring defect appears at 29.06 Hz (−165.98 dB) and motor shaft unbalance appears at 44.87 Hz with an amplitude of −195.83 dB. Flywheel unbalance, which is around 7.12 Hz with an amplitude of −172.46 dB, generates five harmonics. Similarly, the belt-driving defect appears at 5.12 Hz with an amplitude of −166.80 dB. For this defect, the second, fourth, and fifth harmonics show up, while the third harmonic is absent. As before, these are not reliable in determining the severity of the fault.

The parametric spectrum of Fig. 20 confirms the appearance of the outer ring defect (29.06 Hz). The other previously detected faults are also present in this spectrum.

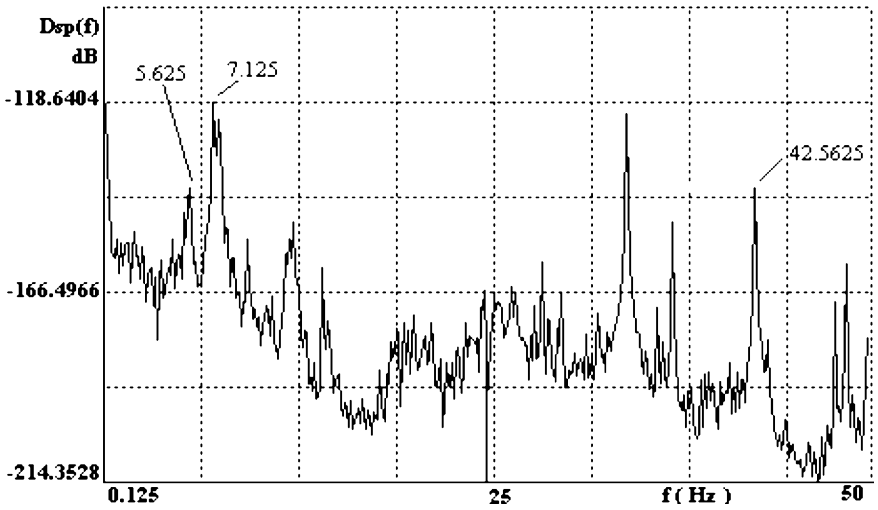

Fig. 17. Conventional spectrum (correlogram).

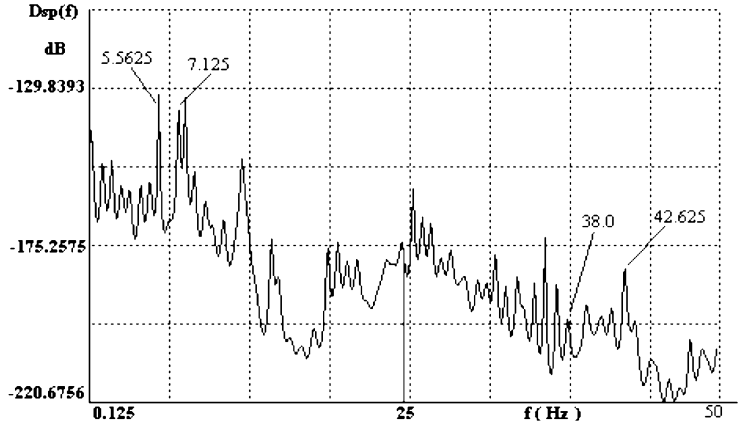

Fig. 18. Parametric spectrum (p order via AIC).

4.4. Discussion

Throughout the experimental work, the number of faults detected increased, and in some cases, the defects were only visible on the parametric spectrum at an early stage. This is because for given measurement parameters (sample number, frequency range, signal-to-noise ratio), parametric spectrum analysis techniques do offer a better resolution over conventional Fourier transform-based methods. As pointed out previously, these so-called high-resolution techniques must be implemented very cautiously due to the associated computational complexity.

Parametric methods should not replace conventional spectrum analysis techniques but complement them when a large spectrum resolution is required, to separate neighboring characteristic spectral peaks, or when the vibratory signature of the entire system has to be recorded and individual components cannot be

Fig. 19. Conventional spectrum (correlogram).

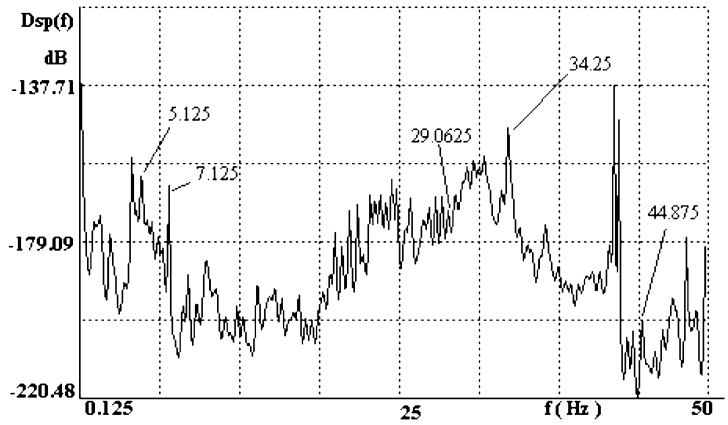

Fig. 20. Parametric spectrum.

Table 3
Characteristic fault frequencies for the "standby" mode of operation

Localised defects	Conventional spectrum			Parametric spectrum		
	Recording 1	Recording 2	Recording 3	Recording 1	Recording 2	Recording 3
Flywheel unbalance	Yes	Yes	Yes	Yes	Yes	Yes
Driving defect	No	Yes	Yes	Yes	Yes	Yes
Motor shaft unbalance	No	No	Yes	Yes	Yes	Yes
Ball defect	No	No	No	No	Yes	Yes
Outer ring defect	No	No	Yes	No	No	Yes
Inner ring defect	No	No	No	No	No	No

monitored. Table 3 illustrates the various characteristic fault frequencies observed throughout the measurement period for each implemented method, for a standby mode of operation of the machine.

5. Conclusions

The problems related to press kinematics do not allow the use of all digital signal processing methods for the detection of defects. Spectrum analysis remains the most efficient tool to localize and monitor the defect condition of various components on an industrial site.

The study reported here has established that parametric techniques along with conventional methods bring additional information, since they display all of the recurring (periodic) signals in a vibratory signature. Hence, the spectrum amplitudes stemming from both methods have not been compared, as the aim of the work was to highlight the presence of characteristic frequencies surrounded by spectral noise. This enables the detection of a fault at an early stage and the monitoring of its evolution over a period of time. Therefore, the technique is worthwhile for monitoring machinery condition.

As a result of machine accessibility restrictions, the measurement period was limited to nine months. This time period was not sufficiently long to detect the evolution of the amplitudes of the characteristic frequencies corresponding to identified faults on the machine.

The press used for the work described here has been operating for more than 20 years and the deterioration of its parts is a slow process. However, the results of the research reported here have indicated components that are becoming damaged and those that are still in good working order. Current research is directed towards the use of an appropriate vibration signal model like the ARMA model that could incorporate correlation between model parameters and the characteristic frequencies contained in the signal. In this case, model parameter evolution monitoring may turn out to be of significant benefit to rotating machinery monitoring.

References

Akaike, H., 1974. A new look at the statistical model identification. IEEE AC 19, 715–723.

Baillie, D.C., Mathiew, J., 1996. A comparison of autoregressive modelling techniques for fault diagnosis of rolling element bearings. Mechanical Systems and Signal Processing 2, 1–17.

Dickie, N, Jr., Nandak 1994. A comparative study of AR order selection méthds. Signal processing 40, 239–255.

Drouiche, K., Sidahmed, M., 1991. GRENIER : détection de défauts d'engrenages par analyse vibratoire. Traitement du signal 8 (5), 331–343.

Kay, S.M., Marple Jr., S.L., 1981. Spectrum analysis – a modern perspective. Proceeding of the IEEE. 69 (11), 81–87.

Mechefske, C., Mathiew, J., 1992. Fault detection and diagnosis in low speed rolling element bearings part I: the use of parametric spectra. Mechanical Systems and Signal Processing 4, 297–3077.

Pachaud, C., Fray, C., 1997. Contribution du facteur de crête et du kurtosis à l'identification des défauts induisant des forces impulsionnelles périodiques. Mécanique industrielle et matériaux 50 (2), 61–69.

Robert, T., Mailhes, C., 1994. Colloque C5 Effet de perturbation sur l'estimation des modèles autoregressifs. Journal de physique 4, 1383–1386.